

Anisotropy of exciton migration in poly(*p*-phenylene vinylene)

D. E. Markov and P. W. M. Blom

Molecular Electronics, Materials Science Centre^{Plus}, University of Groningen, Nijenborgh 4, NL-9747 AG Groningen, The Netherlands

(Received 9 February 2006; revised manuscript received 29 June 2006; published 16 August 2006)

The dynamics of the exciton transport in poly(*p*-phenylene vinylene) (PPV) blended with a low concentration of fullerene molecules is monitored by time-resolved photoluminescence measurements. The diffusion driven motion of excitons toward these scavengers is modeled using a theory based on a random walk of a particle on lattice sites with traps. From this analysis an exciton diffusion constant of $(4 \pm 0.5) \times 10^{-4} \text{ cm}^2/\text{s}$ and a diffusion length of 7 nm are obtained. These exciton transport parameters are equivalent to results obtained in bilayer polymer/fullerene heterostructures, demonstrating that the exciton dynamics in PPV are dominated by a one-dimensional migration perpendicular to the film.

DOI: [10.1103/PhysRevB.74.085206](https://doi.org/10.1103/PhysRevB.74.085206)

PACS number(s): 78.66.Qn, 78.20.Bh, 78.47.+p

I. INTRODUCTION

Conjugated polymers are currently seen as attractive materials for optoelectronic applications as light-emitting diodes and solar cells. Excitonic processes play an important role in the operation of these polymer-based devices. In particular, the migration of excitons in the conjugated polymer phase of bulk heterojunction polymer:fullerene photovoltaic (PV) cells^{1,2} is crucial for harvesting of photons: the length of exciton diffusion sets a limit to the characteristic size of the polymer phase in this type of PV cells. In polymer light-emitting diodes (PLEDs) based on poly(*p*-phenylene vinylene) (PPV) derivatives, it has been demonstrated that a metallic cathode effectively quenches the electroluminescence (EL) by photoexcitation energy transfer from the polymer to the metal.³ The resulting exciton depletion zone at the cathode is further enlarged by migration of excitons toward this exciton quenching sink, thereby enhancing the EL quenching and reducing the device efficiency.⁴ An important difference is that in a bulk heterojunction excitons in the polymer phase can carry out a three dimensional (3D) migration towards the fullerene interface, whereas in a PLED the excitons migrate towards the cathode in the direction orthogonal to the plane of the thin film. Understanding of the nature and dimensionality of exciton migration in thin films of conjugated polymers is therefore of crucial importance. The optical properties of spin-coated conjugated polymer films are known to exhibit a significant anisotropy, pointing to a preferential alignment of the chains in the plane of the film.^{3,5,6} Consequently, a dominance of either intrachain or interchain energy transfer will lead to a strong anisotropy of the exciton migration in thin conjugated polymer films.

From excited state decay studies in an artificial system consisting of a conjugated polymer encapsulated into the channels of mesoporous silica glass, it has been suggested that intrachain energy transfer is slower than interchain.^{7,8} The latter is more rapid because of the granted much better physical proximity of polymer segments in the direction orthogonal to the chain. However, this conclusion is contrary to previous interpretations of anisotropy decay data obtained in solutions and films of conjugated polymers, which suggested a fast initial exciton hopping step most likely to occur along the polymer backbone in the film as well as in solution.⁹⁻¹¹

Conjugated polymers can be considered as arrays of chromophores consisting of fully conjugated segments of the polymer chains of varying length, separated by breaks in conjugation due to kinks and chemical defects.¹² It is generally accepted that energy migration in conjugated polymer films can be understood in terms of an incoherent hopping motion of neutral photoexcitations between the different sites of the polymer.¹³ Two mechanisms of the energy transfer have been considered: dipole-dipole coupling (Förster transfer) and phonon-assisted tunneling (Miller-Abrahams type). Monte Carlo (MC) simulations of the transient luminescence in PPV films showed that the exciton dynamics on the time scale of several hundred picoseconds to nanoseconds are very sensitive to the choice of the transfer mechanism.¹³ Assuming transfer via dipole-dipole coupling resulted in a much faster luminescence decay than observed experimentally, whereas a better agreement was achieved using exciton hopping rates with an exponential distance dependence. However, in these simulations the exciton dynamics were considered to be of a three-dimensional isotropic nature and the dimensionality of exciton migration was not addressed.

Recently, we have studied exciton diffusion in PPV derivatives by means of time-resolved luminescence spectroscopy.^{14,15} Exciton dynamics has been monitored on the time scale of several hundred picoseconds in a bilayer model system, consisting of conjugated polymer film spin-cast on top of a fullerene layer. The fullerene molecules were immobilized via a polymerization reaction, leading to a well-defined and sharp polymer/fullerene interface. Since the chains of the conjugated polymers are mostly aligned in the plane of the substrate, the dynamics of the photoluminescence is expected to be mainly governed by exciton migration between adjacent conjugated segments of different chains (interchain) in the direction orthogonal to the quenching fullerene interface. Thus, photoluminescence quenching in this bilayer model system, as schematically shown in Fig. 1(a), serves as a probe for the interchain exciton dynamics, characterized by a one-dimensional diffusion constant D . For poly[2-(4-(3',7'-dimethyloctyloxyphenyl))-co-2-methoxy-5-(3',7'-dimethyloctyloxy)-1,4-phenylene vinylene] (NRS-PPV) an exciton diffusion constant of $3 \times 10^{-4} \text{ cm}^2/\text{s}$ has been obtained.

In order to further assess the dimensionality of the exciton migration in PPV we present time-resolved luminescence

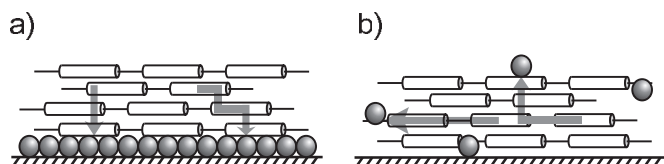


FIG. 1. Schematic geometry of the two model systems: (a) Polymer/fullerene bilayer heterostructure (1D); (b) polymer:fullerene blend (3D).

measurements on identical conjugated polymer films but now blended with a low concentration of fullerene molecules. The randomly distributed fullerene molecules serve as exciton quenching centers. As schematically shown in Fig. 1(b) this experimental geometry mimics exciton capture upon diffusion in three dimensions (3D). We find that the 3D energy migration in films of this PPV-based copolymer is quantitatively described with a random walk model in which the excitons predominantly migrate in one dimension (1D). The diffusion constant obtained for this preferred direction of exciton migration is identical to the one found previously in the polymer/fullerene bilayer model system.¹⁴ This demonstrates that the exciton migration in a PPV thin film is dominated by energy transfer perpendicular to the film. This behavior of exciton migration is in accordance with the reported dominance of the interchain energy transfer over intrachain hopping⁸ combined with the existence of the preferential alignment of the polymeric chains upon spin-processing of conjugated polymers.^{3,5,6}

II. EXPERIMENT

For the preparation of the polymer:fullerene blend films, stock solutions of NRS-PPV (Ref. 15) and the soluble fullerene derivative—[6,6]-phenyl C₆₁-butyric acid methyl ester (PCBM) in toluene were prepared. Then, the PCBM solution was titrated into the NRS-PPV solution and the PCBM concentration was varied from 0 to 6 w%. Subsequently, these solutions with low PCBM concentrations were spin-coated on top of a glass substrate. This resulted in NRS-PPV films with the incorporated PCBM molecules separated by average distances ranging typically from 2 to 7 nm. The films were prepared in the glovebox under nitrogen atmosphere to minimize carbonyl defects, and the film thicknesses typically amount to 100 nm. Figure 1(b) schematically represents a sample configuration, used in our study.

PCBM molecules are known to quench conjugated polymer luminescence by efficient electron transfer from the polymer to the fullerene, and thus act as exciton scavengers.^{16,17} Photoinduced short-range electron transfer from the conjugated polymer to the fullerene is highly efficient and occurs with a characteristic time of 45 fs.^{17–19} Time-resolved luminescence quenching was monitored as a function of PCBM concentration (quencher spacing distance) in NRS-PPV films. Time-resolved optical experiments were carried out with the frequency doubled output of a mode-locked femtosecond Ti:sapphire laser. The polymer excitation was performed at 400 nm, with *p*-polarized light at 64° incident angle in order to minimize internal reflections. Typi-

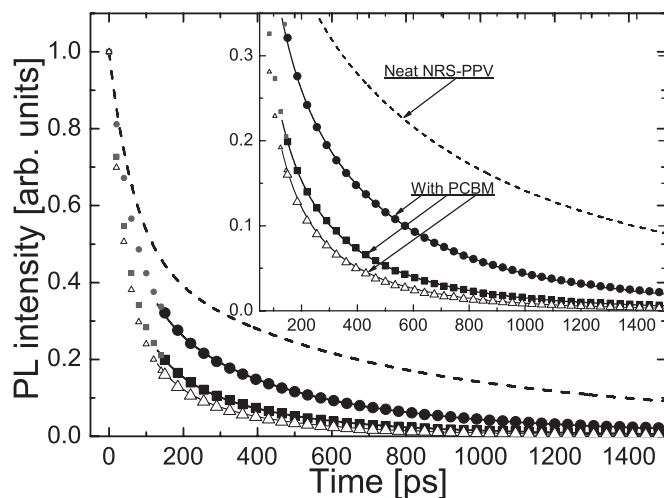


FIG. 2. Luminescence decay curves for a neat NRS-PPV (dashed curve) and for NRS-PPV:PCBM films of three PCBM concentrations: 0.43 w% (●), 0.86 w% (■), and 1.3 w% (△). Solid lines are fits to Eq. (1) giving the exciton diffusion constant of the order of 4×10^{-4} cm²/s (solid curves). The inset magnifies a fitting area.

cal time-averaged excitation intensities on the sample were about 30 mW/cm². Exciton-exciton “bimolecular” quenching interactions are ruled out at this excitation condition as the exciton densities are well below the threshold for amplified spontaneous emission or exciton-exciton annihilation.^{20,21} Emission was collected normal to the excitation beam, at 580 nm, which corresponds to the maximum of the polymer luminescence spectrum. To avoid degradation, samples were sealed under nitrogen in a cell with a quartz window. In time-correlated single photon counting (TCSPC) experiments²² an instrument response function of 30 ps (full width at half maximum) was used for the deconvolution of the luminescence decay. All optical experiments were performed at room temperature.

III. RESULTS AND DISCUSSION

Time-resolved photoluminescence (PL) experiments were performed to study the exciton decay dynamics for various PCBM concentrations in NRS-PPV films. Figure 2 presents deconvoluted and normalized PL decay data for a neat polymer film (dashed curve) and for NRS-PPV:PCBM films of three PCBM concentrations: 0.43, 0.86, and 1.3 w% (symbols). The excitons generated in the polymer by pulsed laser excitation reach the PCBM molecules, being dispersed in the polymer film, by diffusive motion over several nanometers. Then the excitons get quenched due to electron transfer from the polymer to the PCBM.^{16,17} This results in a faster PL decay as compared to the neat polymer PL decay. An increase of the PCBM concentration reduces the average distance between the PCBM molecules, and enhances the probability for an exciton to reach such a quenching center. This leads to an increase of the PL quenching and a faster PL decay, as shown in Fig. 2. For PCBM concentrations lower than 0.4 w%, meaning that the exciton quenchers are sepa-

rated by distances larger than the characteristic exciton diffusion length (~ 7 nm),¹⁴ the PL quenching is so small that it does not allow a reliable quantitative analysis of the exciton dynamics. On the other hand, for PCBM concentrations exceeding 2 w% all PL is quenched. Our study therefore focuses on PCBM concentrations in the 0.4–2 w% range.

As a next step we want to extract the exciton migration parameters from the experimental PL decays of Fig. 2 by modeling the diffusion of excitons to the quenching sites in the polymer film. The diffusion considered in this study is a slow activated process of exciton hopping between the chain segments, which occurs upon fast subpicosecond thermalization within an inhomogeneously broadened density of excitonic states.^{23–25}

As shown by Bässler and co-workers depopulation of high-energy excitonic states and “filling up” states below the center of density of states (DOS) directly after excitation is of major importance on the time scale of several picoseconds.¹³ On the time scale of hundred picoseconds, stretched exponential dynamics of the luminescence, detected for states lying deep in the low-energy tail of the DOS, are mostly governed by a slow activated process of exciton hopping between the chain segments. From Monte Carlo simulations it is obtained that at these energies exciton dynamics are dominated by the exciton diffusion toward traps. However, modeling results critically depend on the choice of the microscopic hopping mechanism. Furthermore, in the modeling, hopping is always assumed to be isotropic. Additionally, there is evidence that interchain polaron pairs are formed,^{26,27} and exciton reformation from back transfer occurs with a distribution of rates resulting in a nonmonoexponential decay.²³ In our study we use a time-dependent exciton lifetime in order to account for the complex intrinsic dynamics of photoluminescence (PL) of the polymer. The PL is detected in its spectral maximum on the time scale of several hundred picoseconds, which corresponds to excitons thermalized on states lying deep in the low-energy tail of the DOS. It should be noted that the nonmonoexponential PL decay of the neat NRS-PPV film is only used as a reference. The exciton diffusion parameters are determined from the difference in dynamics with and without quenching centers. In an earlier study we have demonstrated that the extracted parameters only very weakly depend on the particular mechanism that is used to describe the neat PPV luminescence.¹⁴

Balagurov and Vaks (BV) have calculated the survival probability of a particle (an exciton) after a time t diffusing in the presence of randomly distributed absorbing traps (PCBM) for the one, two (2D), and three-dimensional case.²⁸ We apply this theory to the case of a structurally and energetically disordered system as PPV, where diffusive motions of excitons deep in the low-energy tail of the DOS is considered. Here energetic relaxation plays a small role and trapping effects prevail. The 1D result of this theory has been previously used to describe the photoexcitation relaxation toward intrinsic recombination centers in polythiophene thin films.²⁹ Later the 1D, 2D, and 3D results of this model have been applied to the photoexcitation dynamics of a PPV derivative in which exciton quenching sites were intentionally introduced by photo-oxidation.³⁰

The theory calculates the survival probability of an exciton that diffuses with a coefficient D in a matrix of quenching sites. The spreading of the spacing distance between the quenching sites is approximated by a Poisson distribution with average distance L . The BV theory predicts that the PL decay dynamics in the limit of a high trap density or at long times [Eq. (2)] is described by a stretched exponential^{29,30} given by

$$I(t) = I(0) \left(\frac{t}{\tau_{diff}} \right)^{1/2} \exp \left(- \frac{t^\beta}{\tau_{diff}^\beta} \right) \exp \left(- \frac{t}{\tau_0(t)} \right), \quad (1)$$

$$t \gg \frac{L^2}{\pi^2 D}, \quad (2)$$

where $\tau_{diff} = [2\pi^2(3/2)^3 D n_{1d}^2]^{-1}$ is a characteristic diffusion time and $n_{1d} \equiv 1/L$ is the one-dimensional density of quenching centers. The exponent β in the stretched exponential equals 1/3, 1/2, and 3/5 for diffusion in the 1D, 2D, and 3D case, respectively.

A complication is that the photoluminescence decay of the neat NRS-PPV is not monoexponential. In order to account for this more complex decay dynamics a time-dependent exciton lifetime $\tau_0(t)$ is used (see Ref. 14 and references therein). Correspondingly, the BV model is adapted by including $\tau_0(t)$ in the last multiplicative term $\exp[-t/\tau_0(t)]$ of Eq. (1), describing the process of radiative and nonradiative decay of the excited state in the neat polymer film (Fig. 2, dashed curve).

The PL decay data, measured in NRS-PPV films with varying PCBM density, were modeled with Eq. (1) using only two free parameters, $I(0)$ and τ_{diff} . The PL decay in the neat NRS-PPV film (Fig. 2, dashed curve) was used as a reference to account for the natural exciton decay, giving the time-dependent lifetime $\tau_0(t)$. Values for τ_{diff} are derived from the fits to the data of Fig. 2 for three different PCBM concentrations in NRS-PPV film (0.43, 0.86, and 1.3 w%) and these are proportional to n_{1d}^{-2} ($\equiv L^{-2} = n_{3D}^{-2/3}$) (Ref. 23). In order to estimate the average distance between the fullerene molecules we used a PCBM molar mass of 900 g, a polymer mass density of 0.91 g/cm³ and we accounted for the fullerene diameter of about 1 nm. For PCBM concentrations of 0.43, 0.86, and 1.3 w% the fullerene-fullerene spacing L was found to be 6.3, 4.8, and 4.1 nm, respectively. These values are applied to the right-hand side of Eq. (2) to test the validity of Eq. (1), yielding 100, 58, and 42 ps for three concentrations, respectively. Consequently, to ensure the fulfillment of the condition described by Eq. (2), only the data in the time range from 150 ps till 1.5 ns are considered in the simulations. Fitting results do not depend on the choice of the time interval, using the 400 ps–1.5 ns interval yields identical results. For the 1D model the experimental data can be accurately fitted with a single exciton diffusion constant of $(4 \pm 0.5) \times 10^{-4}$ cm²/s. Analysis of the PL decay data for PCBM concentrations higher than 1.3 w% is complicated since most of the polymer PL is quenched within several tens of picoseconds. Another complication would arise from the finite delocalization size of an exciton, which can become significant in comparison with fullerene-fullerene spacing L

TABLE I. Exciton diffusion parameters derived from modeling bilayer and blend structures.

	D [10^{-4} cm ² /s]	L_D [nm]
Bilayer, ^a 1D model	3	6
Blend, BV 1D model	4	7
Blend, BV 2D model	0.6	2.5
Blend, BV 3D model	0.3	2

^aReference 14.

at high PCBM concentrations, while the BV model only accounts for pointlike excitons.

Combining the exciton diffusion constant with the the time-average of the (time-dependent) lifetime $\langle\tau\rangle$ we estimate a value of 7 ± 1 nm for the exciton diffusion length L_D from (Ref. 14)

$$L_D = \sqrt{D\langle\tau\rangle}, \quad (3)$$

where $\langle\tau\rangle$ (1.25 ns) is found from the PL decay curve $I(t)$ for the neat NRS-PPV film (Ref. 14):

$$\langle t \rangle = \frac{\int_0^\infty t \cdot I(t) dt}{\int_0^\infty I(t) dt} \quad (4)$$

The two- and three-dimensional solutions of the BV model also provide satisfactory fits to the data with exciton diffusion parameters, as shown in Table I. Also shown in Table I are the exciton diffusion parameters as obtained from the PL dynamics in well-defined NRS-PV/fullerene heterostructures [Fig. 1(a)].¹⁴ This diffusion coefficient describes the 1D transport of excitons in the direction orthogonal to the plane of the films [Fig. 1(b)] and serves a lower limit for the diffusion constant that is expected to be found in the 'blend' experiment. When the exciton migration in plane of the film, as schematically indicated by the horizontal arrows in Fig. 1(b), dominates over the diffusion normal to the film, the 1D analysis of the PL quenching in polymer:fullerene blends would lead to a significantly higher diffusion coefficient than found in the heterostructure experiment. When both in-plane and normal migrations are of equal magnitude a 2D or even a 3D analysis of the PL quenching would result in an equal number as found in the heterostructure. Finally, a dominance of exciton migration normal to the film, indicated by the vertical arrows in Fig. 1(b), leads to a mainly one-dimensional movement of excitons with the 1D analysis giving identical numbers as the heterostructure measurements. It is evident that in all cases the heterostructure result for D and L_D represent a lower limit for either the 1D, 2D, or 3D analysis.

As seen in Table I we find that the exciton diffusion parameters as extracted from the 1D BV model are nearly equal to the heterostructure data, representing the 1D exciton migration normal to the film. However, the increase in the dimensionality of the model, when modeling exciton diffusion and capture in these blend structures, results in a dramatic

reduction of the derived values for the exciton diffusion constant D (one order of magnitude). Correspondingly, the typical exciton diffusion length L_D decreases down from 7 nm to values of ~ 2 nm. Since these numbers are smaller than the heterostructure limit they can be regarded as unphysically small. Furthermore, such a small L_D is in strong contradiction with the relatively high efficiencies of polymer/fullerene heterostructure photovoltaic devices.³¹ The close agreement between exciton diffusion constants found from the experiments in the heterostructure (3×10^{-4} cm²/s) and blend (4×10^{-4} cm²/s) model systems demonstrates that the exciton migration in PPV is dominated by energy transfer normal to the polymer film.

Assuming most of the polymer chains aligned parallel to the layer,^{3,5,6} this suggests that the exciton migration is governed by interchain hopping between conjugated segments on different polymer chains. The dominance of interchain exciton transport is in qualitative agreement with the result derived from conjugated polymers that are aligned and encapsulated into the channels of mesoporous silica glass.⁸ It was suggested that the interchain energy transfer is efficient since it only requires the physical proximity of polymer segments that are dipole-dipole coupled.⁷ The fact that we observe that exciton migration is essentially of one-dimensional nature suggests that the aromatic and sidegroups of the polymer chains are preferentially aligned inplane with the substrate upon spinprocessing of the polymer films.^{6,32} Interchain distances in the in-plane dimension are then controlled by the sidegroups and are several times larger as compared to the direction normal to the plane, which results in a preferentially 1D migration of excitons by Förster transfer.

It should be noted that the dominance of exciton diffusion perpendicular to the plane of the film, as observed for NRS-PPV, will depend on the chemical structure of the polymer. For example, the nature and lengths of sidechains influence the π - π stacking and energy transfer in various directions, thereby strongly influencing the exact contribution of each dimension. Furthermore, although polymeric chains preferentially align in the plane of the film upon spincoating, there is a significant portion (15%) of conjugated segments oriented perpendicular to the film plane.³ As a result exciton migration in the plane of the film also will be present. However, the equivalence of the exciton dynamics in the bilayer heterostructure and blend shows that for this materials system exciton migration is dominated by diffusion normal to the plane of the film.

IV. CONCLUSIONS

In conclusion, we have studied the anisotropy of the exciton diffusion in a PPV derivative by monitoring the time-

resolved luminescence in polymer:fullerene blend model systems, where exciton scavengers (fullerene) are randomly distributed in three dimensions. The decay of the luminescence for different fullerene densities is described by a theory based on a one-dimensional random walk and an exciton diffusion coefficient of $(4 \pm 0.5) \times 10^{-4}$ cm²/s has been derived. The equivalence of exciton diffusion parameters obtained from bilayer and blend polymer/fullerene model systems shows that exciton migration in PPV occurs in one

dimension perpendicular to the film, suggesting a dominance of an interchain exciton energy transfer.

ACKNOWLEDGMENTS

This work is a part of the research program of the Stichting voor Fundamenteel Onderzoek der Materie [FOM, financially supported by the Nederlandse Organisatie voor Wetenschappelijk Onderzoek (NWO)].

-
- ¹G. Yu and A. J. Heeger, *J. Appl. Phys.* **78**, 4510 (1995).
²J. J. M. Halls, C. A. Walsh, N. C. Greenham, E. A. Marseglia, R. H. Friend, S. C. Moratti, and A. B. Holmes, *Nature (London)* **376**, 498 (1995).
³H. Becker, S. E. Burns, and R. H. Friend, *Phys. Rev. B* **56**, 1893 (1997).
⁴D. E. Markov and P. W. M. Blom, *Appl. Phys. Lett.* **87**, 233511 (2005).
⁵C. M. Ramsdale and N. C. Greenham, *Adv. Mater. (Weinheim, Ger.)* **14**, 212 (2002).
⁶D. McBranch, I. H. Campbell, D. L. Smith, and J. P. Ferraris, *Appl. Phys. Lett.* **66**, 1175 (1995).
⁷B. J. Schwartz, *Annu. Rev. Phys. Chem.* **54**, 141 (2003).
⁸T. Q. Nguyen, J. Wu, V. Doan, B. J. Schwartz, and S. H. Tolbert, *Science* **288**, 652 (2000).
⁹A. Ruseckas, M. Theander, L. Valkunas, M. R. Andersson, O. Inganäs, and V. Sundström, *J. Lumin.* **76-77**, 474 (1998).
¹⁰A. Watanabe, T. Kodaira, and O. Ito, *Chem. Phys. Lett.* **273**, 227 (1997).
¹¹J. Z. Zhang, M. A. Kreger, Q.-S. Hu, D. Vitharana, L. Pu, P. J. Brock, and J. C. Scott, *J. Chem. Phys.* **106**, 3710 (1997).
¹²U. Rauscher, H. Bässler, D. D. C. Bradley, and M. Hennecke, *Phys. Rev. B* **42**, 9830 (1990).
¹³M. Scheidler, U. Lemmer, R. Kersting, S. Karg, W. Riess, B. Cleve, R. F. Mahrt, H. Kurz, H. Bässler, E. Gobel, and P. Thomas, *Phys. Rev. B* **54**, 5536 (1996).
¹⁴D. E. Markov, J. C. Hummelen, P. W. M. Blom, and A. B. Sieval, *Phys. Rev. B* **72**, 045216 (2005).
¹⁵D. E. Markov, C. Tanase, P. W. M. Blom, and J. Wildeman, *Phys. Rev. B* **72**, 045217 (2005).
¹⁶N. S. Sariciftci and A. J. Heeger, *Int. J. Mod. Phys. B* **8**, 237 (1994).
¹⁷C. J. Brabec, G. Zerza, G. Cerullo, S. De Silvestri, S. Luzzati, J. C. Hummelen, and S. Sariciftci, *Chem. Phys. Lett.* **340**, 232 (2001).
¹⁸E. Peeters, P. A. van Hal, J. Knol, C. J. Brabec, N. S. Sariciftci, J. C. Hummelen, and R. A. J. Janssen, *J. Phys. Chem. B* **104**, 10174 (2000).
¹⁹J. G. Muller, J. M. Lupton, J. Feldmann, U. Lemmer, M. C. Scharber, N. S. Sariciftci, C. Brabec, and U. Scherf, *Phys. Rev. B* **72**, 195208 (2005).
²⁰G. J. Denton, N. Tessler, N. T. Harrison, and R. H. Friend, *Phys. Rev. Lett.* **78**, 733 (1997).
²¹N. Tessler, G. J. Denton, N. T. Harrison, M. A. Stevens, S. E. Burns, and R. H. Friend, *Synth. Met.* **91**, 61 (1997).
²²J. N. Demas, *Excited State Lifetime Measurements* (Academic Press, New York, 1983).
²³L. J. Rothberg, M. Yan, F. Papadimitrakopoulos, M. E. Galvin, E. V. Kwock, and T. M. Miller, *Synth. Met.* **80**, 41 (1996).
²⁴R. Kersting, U. Lemmer, R. F. Mahrt, K. Leo, H. Kurz, H. Bässler, and E. O. Gobel, *Phys. Rev. Lett.* **70**, 3820 (1993).
²⁵R. F. Mahrt, U. Lemmer, A. Greiner, Y. Wada, H. Bassler, E. O. Gobel, R. Kersting, K. Leo, and H. Kurz, *J. Lumin.* **60**, 479 (1994).
²⁶J. W. P. Hsu, M. YAN, T. M. Jedju, L. J. Rothberg, and B. R. Hsieh, *Phys. Rev. B* **49**, 712 (1994).
²⁷M. Gailberger and H. Bassler, *Phys. Rev. B* **44**, 8643 (1991).
²⁸B. Ya. Balagurov and V. G. Vaks, *Sov. Phys. JETP* **38**, 968 (1974).
²⁹G. S. Kanner, X. Wei, B. C. Hess, L. R. Chen, and Z. V. Vardeny, *Phys. Rev. Lett.* **69**, 538 (1992).
³⁰M. Yan, L. J. Rothberg, F. Papadimitrakopoulos, M. E. Galvin, and T. M. Miller, *Phys. Rev. Lett.* **73**, 744 (1994).
³¹J. J. M. Halls, K. Pichler, R. H. Friend, S. C. Moratti, and A. B. Holmes, *Appl. Phys. Lett.* **68**, 3120 (1996).
³²Y. Shi, J. Liu, and Y. Yang, *J. Appl. Phys.* **87**, 4254 (2000).